Phytomedicine 22 (2015) 981–992

Contents lists available at ScienceDirect

Phytomedicine

journal homepage: www.elsevier.com/locate/phymed

Synergy assessment of fixed combinations of Herba Andrographidis and Radix Eleutherococci extracts by transcriptome-wide microarray profiling

Alexander Panossian[a,*], Ean-Jeong Seo[b], Georg Wikman[a], Thomas Efferth[b]

[a] Swedish Herbal Institute Research and Development, Askloster, Sweden
[b] Department of Pharmaceutical Biology, Institute of Pharmacy and Biochemistry, Johannes Gutenberg University, Mainz, Germany

ARTICLE INFO

Article history:
Received 24 July 2015
Revised 5 August 2015
Accepted 11 August 2015

Keywords:
Acanthaceae
Araliaceae
Network pharmacology
Pharmacogenomics
Synergy
Venn diagrams

ABSTRACT

Background: Generally accepted, but insufficiently proved, the concept of synergy is based on an assumption that combining of two biologically active substances is justified because the combination is more active and less harmful than the ingredients.
Hypothesis: Analysis of RNA microarray of isolated neuroglia cells and the comparison the number of genes deregulated by plant extracts and their fixed herbal formulation might be a useful tool/method for assessment of synergistic and antagonistic interactions of herbal extracts in human organism.
Aim: The primary aim of this study was to extend a new method of assessment of synergistic and antagonistic interactions of herbal extracts in isolated human neuroglia cells when they applied in the form of fixed combinations. The secondary aim of the study was to predict possible effects of Herba Andrographidis (APE), Radix Eleutherococci (ESE) genuine extracts and their fixed combination Kan Jang (KJ) on cellular and physiological functions and associated diseases. The third task of the study was to find evidences that justify the hypothesis that these plants extracts in combination are more useful than the monodrugs.
Methods: Gene expression profiling was performed on the human neuroglia cell line T98G after treatment with APE, ESE, KJ and total number of more than two fold-deregulated genes from all experiments were compared by Venn diagram. Interactive pathways downstream analysis was performed with data sets of significantly up– or down-regulated genes and predicted effects on cellular functions and diseases were identified by Ingenuity IPA database software.
Results: ESE and APE significantly deregulate 207 and 211 genes correspondingly; 36 deregulated genes were common for both extracts. In total of 382 deregulated genes was expected to be deregulated by their fixed combination KJ. However, it was found only 250 genes deregulated by KJ. Among these 250 genes, 111 genes were unique for the KJ combination and not affected by ESE and APE. This is presumably due to synergistic interactions of molecular networks affected by ESE and APE. Meanwhile, 170 genes deregulated by ESE, and 55 genes deregulated by APE when tested alone, were not up- or downregulated by KJ. That is the result of antagonistic integrations of ESE and APE extracts when applied in the combination. Fold change of expression of 18 common genes deregulated by APE, ESE and KJ was not additive when APE and ESE are combined in KJ herbal formula. However, a qualitative difference is observed in the fingerprint of deregulated genes of daughter substance (KJ) compared to fingerprints/signatures of deregulated genes of parent substances (APE and ESE).

Specific for KJ and predictable (z-score > 2) were the effects on pathways and networks associated with infectious and chronic inflammatory disorders, namely encephalitis or neurological movement disorders. Noteworthy, Eleutherococcus alone has no effect on those networks, particularly on encephalitis network, while KJ deregulates 11 genes which have predictable inhibitory effect on infection, while APE regulates

Abbreviations: APE, *Andrographis paniculata* L. Nees. (herb) genuine extract; EL, eleutherosides B and E; ESE, *Eleutherococcus senticosus* (Rupr. & Maxim.) Maxim. (root) genuine extracts; IPA, Ingenuity Pathway Analysis software; KJ, Kan Jang fixed combination of APE and ESE.

* Corresponding author. Tel.: +46702818171; fax: +46 430 23723.
E-mail address: alexander.panossian@shi.se, ap.phytomedicine@gmail.com (A. Panossian).

http://dx.doi.org/10.1016/j.phymed.2015.08.004

only 5 genes which are activated in encephalitis. It can be speculated that APE in combination with ESE may have better therapeutic effect, since more targets are affected. Similar suggestion is justified regarding neurological movement, which is associated with chronic inflammation, like arthritis and osteoarthrosis. Though, microarray analysis did not provide final proof that the genes induced by the KJ, APE and ESE are responsible for the physiological effects observed in humans following their oral administration. It provided insights into putative genes and directions for future research and possible implementation into practice.

The most significantly affected canonical pathways deregulated by KJ and APE was interferon signaling pathway, indicating the possible effectiveness of KJ and APE in the treatment of severe sepsis, systemic lupus erythematosus and other autoimmune diseases

Conclusion: Analysis of RNA microarray data from isolated neuroglia cells and the comparison the number of genes deregulated by plant extracts and their fixed herbal formulation might be a useful tool/method for assessment of synergistic and antagonistic interactions of herbal extracts in human organism. Combination of APE and ESE in KJ formulation is most likely justified.

Introduction

The idea to combine two or more plant extracts in one presumably more effective combination traced back many centuries. There are numerous examples of complex formulations widely used in traditional Chinese medicine and other traditional medicines worldwide.

The generally accepted, but insufficiently proved concept of synergy is based on the assumption that combining two substances, which act on different molecular targets in cells, may result in additive or supra-additive responses in cells or organisms, due to synergistic interactions of molecular targets within their molecular networks (Wagner 2006; Efferth and Koch 2011). *A priori* accepted is also the assumption that fixed combinations have the same characteristic features as their single constituents. In other words, at least additive effects can be expected for fixed combinations. However, our recent study (Panossian et al. 2013) showed that it is actually not true: the combination of three plant extracts may not exhibit some effects that single ingredients have. At the same time, it may exert some new and unique features, which the constituents do not reveal.

In this article, we extend this observation to another combination of plant extracts and explore a novel method of synergy assessment of herbal extracts in their fixed combination. The method is based on the analysis of transcriptome-wide microarray-based mRNA expression profiling as previously described by us for the first time (Panossian et al. 2013). In that study, isolated brain cells were separately incubated with three plant extracts, Rhodiola, Eleuterococcus and Schisandra or their fixed combination (Panossian et al. 2013). The total numbers of more than two fold-deregulated genes from all experiments were compared by Venn diagram. The number of genes deregulated by the combination, but not by any constituent alone provided evidence of synergistic interaction of the ingredients in the fixed combination. This is actually the essence of the new analysis method of synergy effects.

In present study, two well-known plants *Andrographis paniculata* L. Nees. (herb), Acanthaceae (Herba Andrographidis 2002) and *Eleutherococcus senticosus* (Rupr. & Maxim.) Maxim. (root), Araliaceae (Radix Eleutherococci 2002; ESCOP Monographs 2003) genuine extracts and their fixed combination, Kan Jang (Panossian and Wikman 2012), standardized for the content of andrographiolides and eleutherosides, were explored.

The leaves and aerial parts of *A. paniculata* have been used for prophylactic and symptomatic treatment of respiratory infections, such as common cold, influenza with fever, sore throat, acute and chronic cough, sinusitis, bronchitis and pharyngotonsillitis (Herba Andrographidis 2002; Herba Andrographis (Chuanxinlian) 2010). Commonly found in tropical and subtropical regions, *A. paniculata* is currently one of the most used medicinal plants in Southeast Asia. As antipyretic treatment, it is effective against a wide variety of infection diseases, including urinary infections with difficult painful urination, tonsillitis, dysentery, edema, bacillary dysentery, bronchitis, carbuncles, colitis, coughs, dyspepsia, malarial and intermittent fever, hepatitis, mouth ulcers, sores, tuberculosis, colic, otitis media, vaginitis, pelvic inflammatory disease, chickenpox, and eczema. The plant is also effective for the treatment of carbuncles, sores, venomous snake bites, ulcers in the mouth or on the tongue, liver disorders, burns and traumatic infections. Remarkably, efficacy was demonstrated in clinical studies for prophylaxis and treatment of upper respiratory infections, such as the common cold, uncomplicated sinusitis, bronchitis and pharyngotonsillitis, urinary tract infections, and acute diarrhea [Herba Andrographidis 2002].

E. senticosus is an adaptogenic plant, which increases the state of non-specific resistance against a wide variety of environmental assaults and emotional conditions (Radix Eleutherococci 2002; ESCOP Monographs 2003; Farnsworth et al. 1985). In TCM, it is used to reinforce *qi*, invigorate the function of the spleen and kidney, and anchor the mind (Radix et Rhizoma seu Caulis Acanthopanacis Senticosi (Ciwaujia) 2005). Moreover, a large body of evidence indicated possible benefits of *Eleutherococcus* in the treatment of URT infections.

Kan Jang (KJ) is a fixed combination, which is known in Scandinavia as the medicinal product “naturmedel” since 1979 and has the “well-established” status in Denmark for the treatment of common cold symptoms (Panossian and Wikman 2012). The clinical efficacy of this combination has been demonstrated in influenza (Kulichenko et al. 2003), sinusitis (Gabrielian et al. 2002), and familial Mediterranean fever (Amaryan et al. 2003). In a recent review article, the clinical efficacy of *A. paniculata* extract and KJ was compared and KJ combination demonstrated to be more efficient than the single plant alone (Panossian and Wikman, 2012).

The primary aim of this study was to show that our previous observation with the ADAPT-232 combination consisting of three plant extracts, Radix Eleutherococci (ESE), Schisandra Fruit (SFE) and Radix and Rhizoma Rhodiolae (RRE) is robust and transferable to other combinations such as KJ. We hypothesize that conclusions about synergy and antagonism are justified by interactive downstream signaling pathway analysis. A secondary task of this study was to identify specific molecular pathways and networks affected by *A. paniculata* and *E. senticosus* genuine extracts and their fixed combination, KJ. Therefore, we analyzed microarray-based transcriptome-wide mRNA expression profiles of the neuroglial cell line T98G after exposure to KJ and its single constituents. The choice of T98G cells for our study was justified in our previous publication (Panossian et al. 2013). Interactive pathways downstream analysis was performed with data sets of significantly up- or down-regulated genes. Effects on relevant cellular functions and diseases were predicted by Ingenuity Pathway Analysis (IPA) software.

Materials and methods

Drugs and chemicals

Pharmaceutical grade standardized extracts of *A. paniculata* and *E. senticosus* genuine extracts and their fixed combination, KJ, were manufactured in accordance to ICH Q7A and EMEA guidelines for Good Agricultural and Collecting Practice (GACP) and Good Manufacturing Practice (GMP) of active pharmaceutical ingredients (API), Fig. 1.

The content of plant extracts and their active markers was the same in all preparations. Working samples used in experiments were prepared by dilution of stock solutions (30 mg/ml, DMSO) Herba Andrographidis, (2.7 mg/ml, DMSO) Radix Eleutherococci genuine extracts and their fixed combination KJ (32.7 mg/ml) with appropriate volumes of phosphate buffered saline solution (PBS). Working solutions of 100 μl were added to 9.9 ml of cell culture to obtain the same final concentrations of active markers and genuine extract as in the incubation media of KJ: 30 μg/ml of HA, 32.7 μg/ml of KJ and 2.7 μg/ml of RE respectively (Table 1)

The concentration of 32.7 μg/ml (final concentration of KJ in incubation media) is based on the results of pharmacokinetic study of KJ -derived andrographolide in human blood plasma, where it was detected in concentrations of ~ 0.7 μg/ml = 2 μM (Panossian et al., 2000).

The concentrations of the total extracts of both herbal ingredients and their active constituents were compatible is all test samples: *e.g.* the final concentration of andrographolide is the same (2 μM, 700 μg/l in all test samples containing andrographolide, namely in HA extract, and KJ. Similarly, eleutheroside E concentrations were calculated based of the results of the HPLC analysis of its content in genuine extracts and KJ combination. The concentrations of genuine extracts have been calculated using specifications of KJ to ensure that they correspond to therapeutically effective doses.

Cell culture

The human neuroglial cell line T98G was purchased from the American Type Culture Collection (ATCC, CRL-1690). Cells were grown in DMEM + GlutaMAX-I (Gibco, Darmstadt, Germany) with 10% fetal bovine serum (Gibco, Darmstadt) and 1% penicillin/streptomycin (Gibco). They were passaged twice a week and maintained in a 37 °C incubator in a humidified atmosphere with 5%

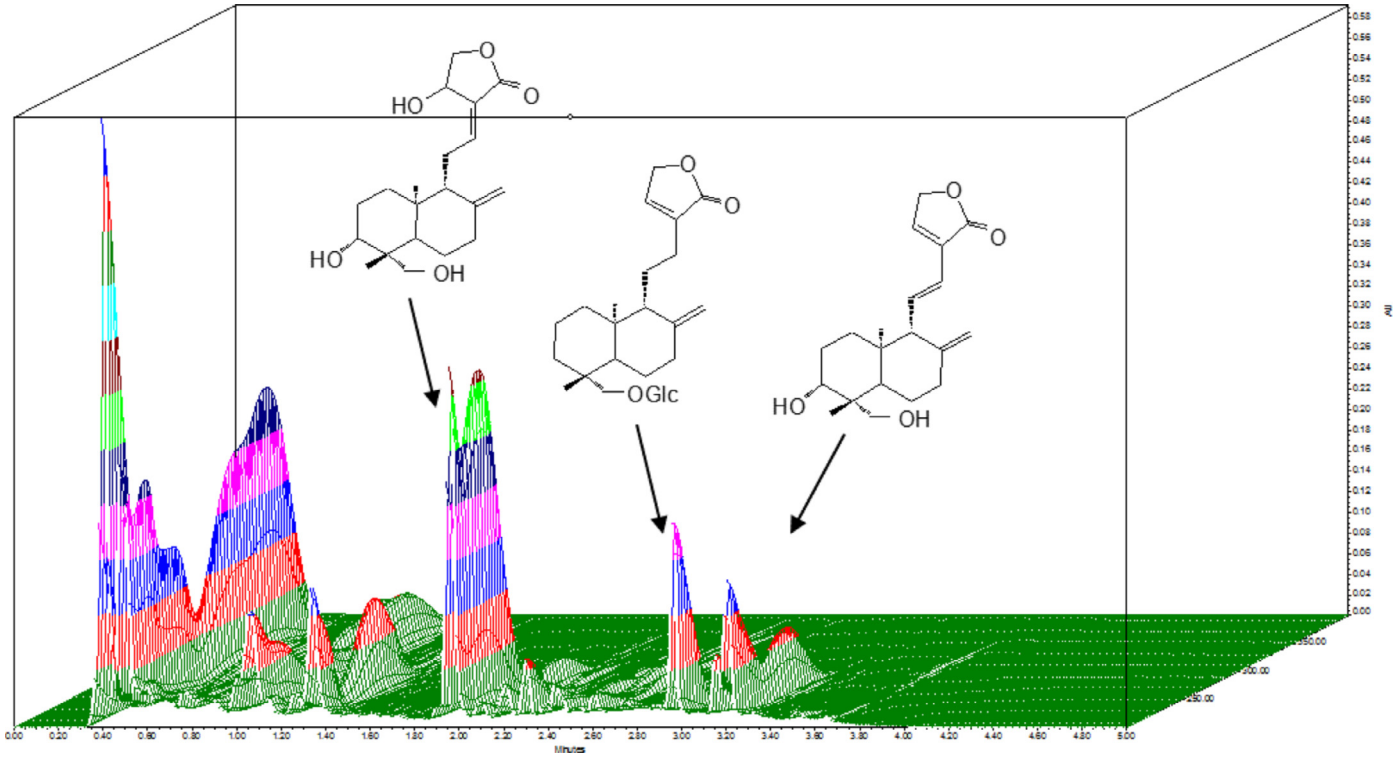

Fig. 1. Three-dimensional HPLC fingerprint of KJ detection from 200 to 400 nm.

Table 1
Concentrations used to treat T98G neuroglial cells for microarray experiments.

Herbal extract	Final concentration, μg/ml	Final concentration of and, μg/ml	mRNA concentration, ng/μl	Amount for microarray, μl; 1 μg	Amount for cDNA, μl; 2 μg
Andrographolide	0.70	0.70 = 2 μM	354.7	2.82	5.64
	0.70	0.70 = 2 μM	323.6	3.09	6.18
APE	30.00	0.70 = 2 μM	357.6	2.80	5.60
	30.00	0.70 = 2 μM	235.3	4.25	8.50
KJ	32.70	0.70 = 2 μM	385.1	2.60	5.20
	32.70	0.70 = 2 μM	327.8	3.05	6.10
ESE	2.70	–	323.0	3.09	6.18
	2.70	–	342.8	2.92	5.84

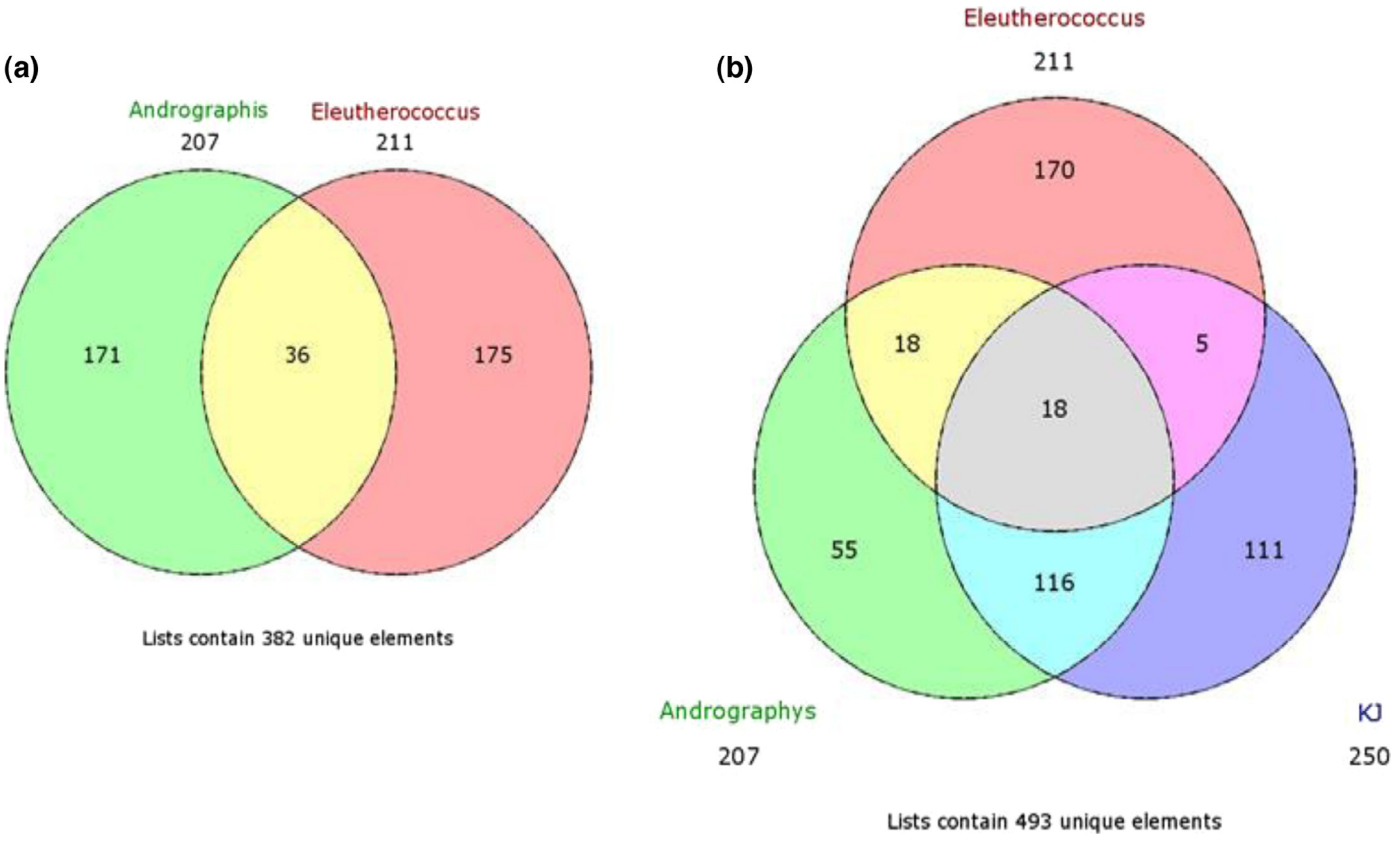

Fig. 2. Venn diagrams of deregulated genes induced by the treatment of neuroglia cells with (a) APE, ESE alone and (b) APE, ESE in KJ. Genes uniquely deregulated by each extract alone (55 by APE and 170 by ESE) and 111 unique genes deregulated by KJ show antagonistic and synergistic interactions of ESE and APE in KJ. Overlapping sections show common genes deregulated by these ingredients in the KJ combination.

Table 2
Expression of genes commonly deregulated by APE, ESE and KJ.

Genes	APE	ESE	KJ	Expected sum
ACOT7	−1.586	−1.516	−1.723	−3.102
APOBEC3F	−1.444	−1.558	−1.647	−3.002
APOBEC3G	−1.619	−1.376	−1.705	−2.995
ASS1	−1.630	−1.366	−1.834	−2.996
CXCL12	***1.564***	***−1.500***	***1.591***	***0.064***
F2RL2	2.211	1.454	2.594	3.665
GBP1	−1.729	−1.464	−1.636	−3.193
GLDN	1.569	1.464	1.772	3.033
HIST1H2AC	−1.765	−1.424	−1.558	−3.189
KRT18	−1.796	−1.591	−2.166	−3.387
LYPD1	−1.699	−1.464	−1.591	−3.163
NAMPT	***1.860***	***−1.647***	***2.151***	***0.213***
PSMB8	−1.597	−1.495	−1.439	−3.092
RCAN1	−1.647	−1.376	−1.444	−3.023
RNY4	2.092	1.361	1.510	3.453
SLC6A1	1.449	1.905	1.586	3.354
SLCO2B1	2.990	1.449	3.238	4.439
SRXN1	2.063	1.361	1.952	3.424

CO_2. All experiments were conducted using cells in the logarithmic growth phase.

Drug treatment

T98G cells were seeded 24 h before treatment on 6-well plates in a density of 150,000 cells per well. The next day, old medium was removed and cells were treated in a final volume of 10 ml.

The ethanol content was 0.8% for cells treated with isolated compounds and vehicle-treated control cells (test sample Z). Two technical replicates were performed for each sample. Cells were incubated with the test substances for 24 h at 37 °C and then subjected to RNA isolation.

mRNA isolation and quality control

Cells were harvested after 24 h of treatment. Total RNA was isolated using InviTrap Spin Universal RNA Mini kit (Stratec Molecular, Berlin, Germany) and dissolved in RNAse free-water. The RNA of the two technical replicates was pooled (1:1) resulting in one sample for each treatment/control. The quality of total RNA was checked by gel analysis using the Total RNA Nano chip assay on an Agilent 2100 Bioanalyzer (Agilent Technologies, Berlin, Germany). All samples were of highest quality with RNA integrity number values of 10.

Gene expression profiling

Microarray hybridizations were performed at the Institute of Molecular Biology (Mainz, Germany). Whole Human Genome RNA chips (8 × 60 K Agilent) were used for gene expression profiling. Probe labeling and hybridization procedures were carried out following the One-Color Microarray-Based Gene Expression Analysis Protocol (http://www.chem.agilent.com/Library/usermanuals/Public/G414090040_GeneExpression_One-color_v6.5.pdf). Briefly, total RNA was labeled and converted to cDNA. Then, fluorescent cRNA (Cyanine 3-CTP) was synthesized and purified using the QIAgen RNeasy Kit (Hilden, Germany). After fragmentation of the cRNA, samples were hybridized for 17 h at 65 °C. Microarray slides were washed and scanned with the Agilent Microarray Scanning system. Images were analyzed and data was extracted. The background was subtracted and

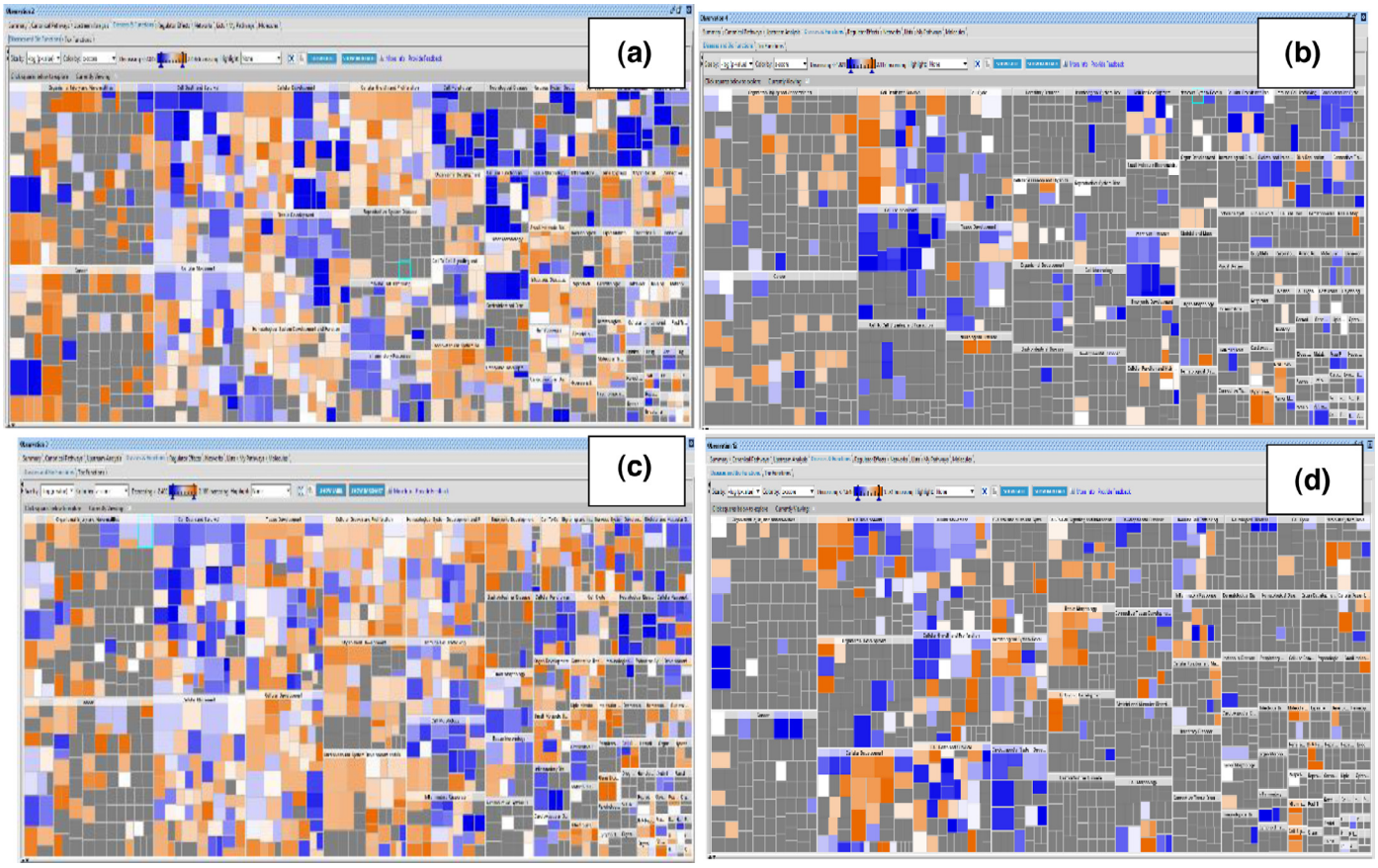

Fig. 3. Conditional "biological signatures" of (a) APE, (b) ESE and (c) KJ; (d) shows new synergy-derived elements of the KJ signature. These windows show the results of downstream effects analysis to visualize biological trends in these experiments and to predict the effect of gene expression changes in these datasets on biological processes and diseases. Color-coded heatmaps identify functions and diseases that are expected to increase or decrease. Details see 'Materials and methods' section.

data was normalized using the standard procedures of Agilent Feature Extraction Software.

Microarray data analysis

Expression data were further analyzed using Chipster software (http://chipster.csc.fi/) to filter genes by varying expression and significance. These steps included filtering genes that were up- or down-regulated by one to three times the standard deviation (depending on the total number of extremely up- or down-regulated genes). A subsequent assessment of significance using empirical Bayes *t*-test further narrowed the pool of genes. All genes further considered showed a significant difference from the control with at least p-value <0.05. Finally, filtered data were subjected to Ingenuity Pathway Analysis for core analysis to determine networks and pathways influenced by the drug treatments (http://www.ingenuity.com/).

Interactive Pathway Analysis (IPA) of complex 'omics' data (http://www.ingenuity.com/)

Downstream effect analysis enables to visualize biological trends in microarray experiments and predicts gene expression changes in these datasets during biological processes. Color-coded heatmaps visualize increased or decreased gene expressions. Downstream effect analysis is based on expected causal effects between genes and functions. The expected causal effects are derived from the literature compiled in the Ingenuity® Knowledge Base. The analysis examines genes in the datasets that are known to affect functions, compares the genes direction of change to expectations derived from the literature. Then, predictions are made for each function based on the direction of change.

The direction of change is the gene expression in the experimental samples relative to a control. If the direction of change is consistent with the literature across most genes, IPA predicts that the function will increase in the experimental sample. Mostly inconsistent with the literature, IPA predicts that the function will decrease in the experimental sample. IPA uses the z-score algorithm to make predictions. The z-score algorithm is designed to reduce the chance that random data will generate significant predictions.

The color of the squares in the heatmap shows the direction of change for the function, based on the regulation z-score:

- Orange – The z-score is positive. IPA predicts that the biological process or disease is trending towards an increase. *Z*-scores ≥ 2 indicate that the function is statistically significantly increased.
- Blue – The *Z*-score is negative. IPA predicts that the biological process or disease is trending towards a decrease. *Z*-scores ≤ -2 indicate that the function is statistically significantly decreased.

The intensity of the colors indicates the prediction strength.

The size of the squares in the heatmap reflects the associated -log of the calculated p-value. Larger squares indicate more significant overlap between the genes perturbed in the dataset and the function or disease. The p-value is a measure of the likelihood that the association between a set of genes in a dataset and a related function is due to random association. The smaller the p-value (which means a larger $-\log$ of that value), the less likely that the association is random and the more significant the association. In general, p-values <0.05 ($-\log = 1.3$) indicate a statistically significant, non-random association.

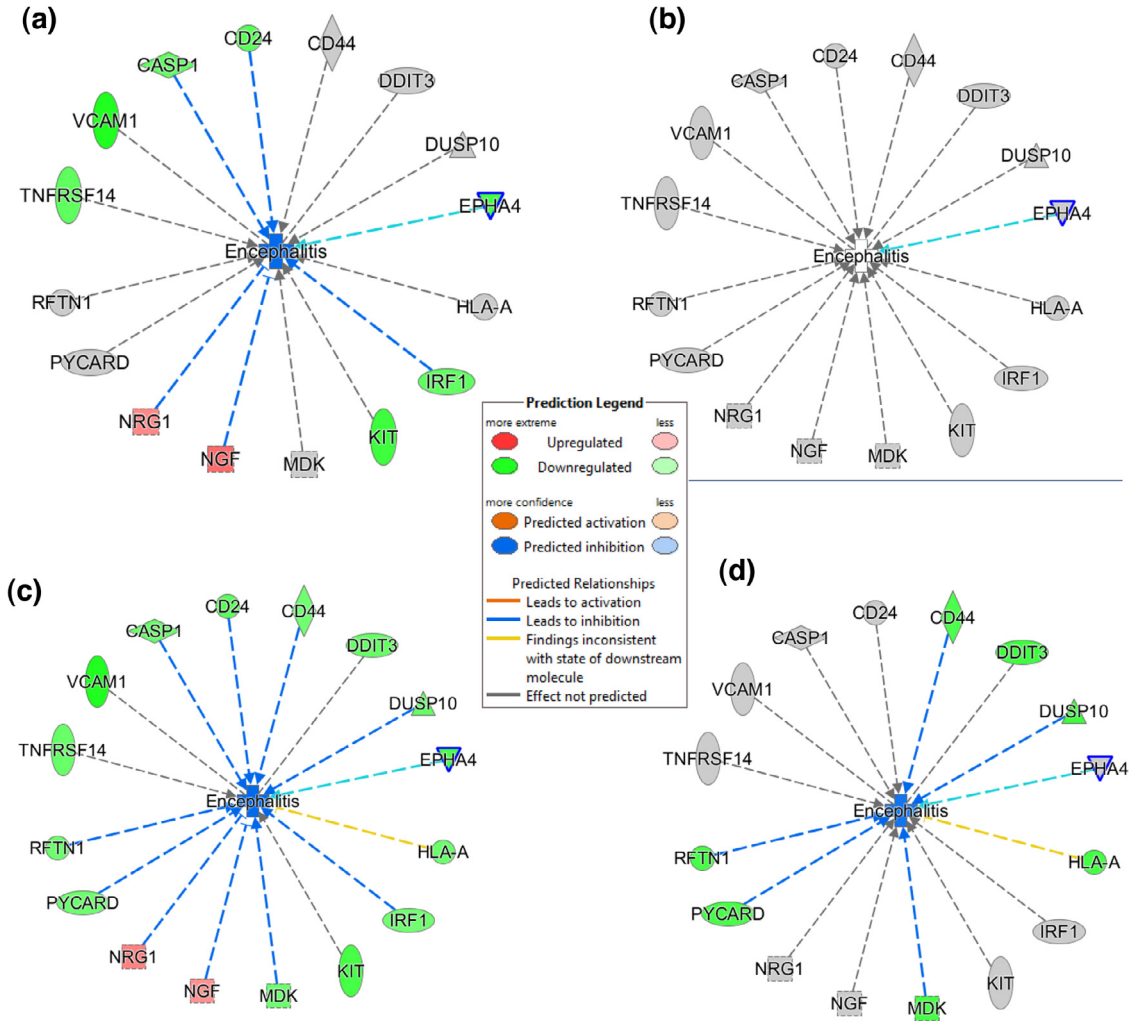

Fig. 4. Predictable effects on molecular networks associated with encephalitis: (a) APE, (b) ESE and (c) KJ; (d) synergy-derived elements of KJ signature.

Venn diagrams

Venn diagrams were generated by software at the websites http://bioinfogp.cnb.csic.es/tools/venny/; http://www.bioinformatics.lu/venn.php; http://bioinformatics.psb.ugent.be/webtools/Venn/.

Results

Effects of single herbal extracts and their fixed combination on mRNA microarray profiles

A microarray-based transcriptome-wide mRNA expression analysis was performed to identify possible targets of the tested substances in T98G cells. The cells were treated with test substances for 24 h in two technical replicates before total RNA was isolated and pooled for microarray hybridization. Significantly deregulated genes were identified compared to untreated controls ($p < 0.05$) by means of Chipster software analysis.

IPA was performed with data sets of significantly up- or down-regulated genes: ESE and APE significantly deregulate 207 and 211 genes correspondingly; 36 deregulated genes were common for both extracts. In total, 382 genes were deregulated by their fixed combination KJ (Fig. 2a). However, only 250 genes were deregulated by KJ (Fig. 2b). Among these 250 genes, 111 genes were unique for the KJ combination and not affected by ESE and APE. This is presumably due to synergistic interactions of molecular networks affected by ESE and APE. Meanwhile, 188 genes deregulated by ESE and 73 genes deregulated by APE, if tested alone. In total, 243 genes were not up- or down-regulated by KJ. This may result from antagonistic integrations of ESE and APE extracts, if applied as combination.

The Venn diagrams in Fig. 2 show the number of uniquely deregulated genes for each extract in comparison to the number of commonly deregulated genes.

The effect of two ingredients on expression of a particular gene is not additive. The fold change of expression of 18 common genes deregulated by KJ was not additive and not the sum of fold changes by APE and ESE as expected, if they were combined in KJ (Table 2). For example, no effect of KJ on *CXCL12* and *NAMPT* genes expression can be predicted based on the sum of the effects of EPE and ESE. However, both of them were upregulated by KJ (Table 2).

However, qualitatively different effects of APE, ESE and their fixed combination KJ was observed for RNA microarray profiles of deregulated genes in T98G cells ("Supplementary" Tables 1 and 2). Synergistic effects of two plant extracts were obvious, when the effects of the combination (KJ) and the single ingredients (APE and ESE) were compared in the mRNA microarray profiles of deregulated genes. This can be illustrated in the corresponding molecular networks (Figs. 4a–d, 5a–f, 6a–e), intracellular signaling pathways (Fig. 7a–c and 8a–e) and predicted effects ("Supplementary" Tables 3 and 4)

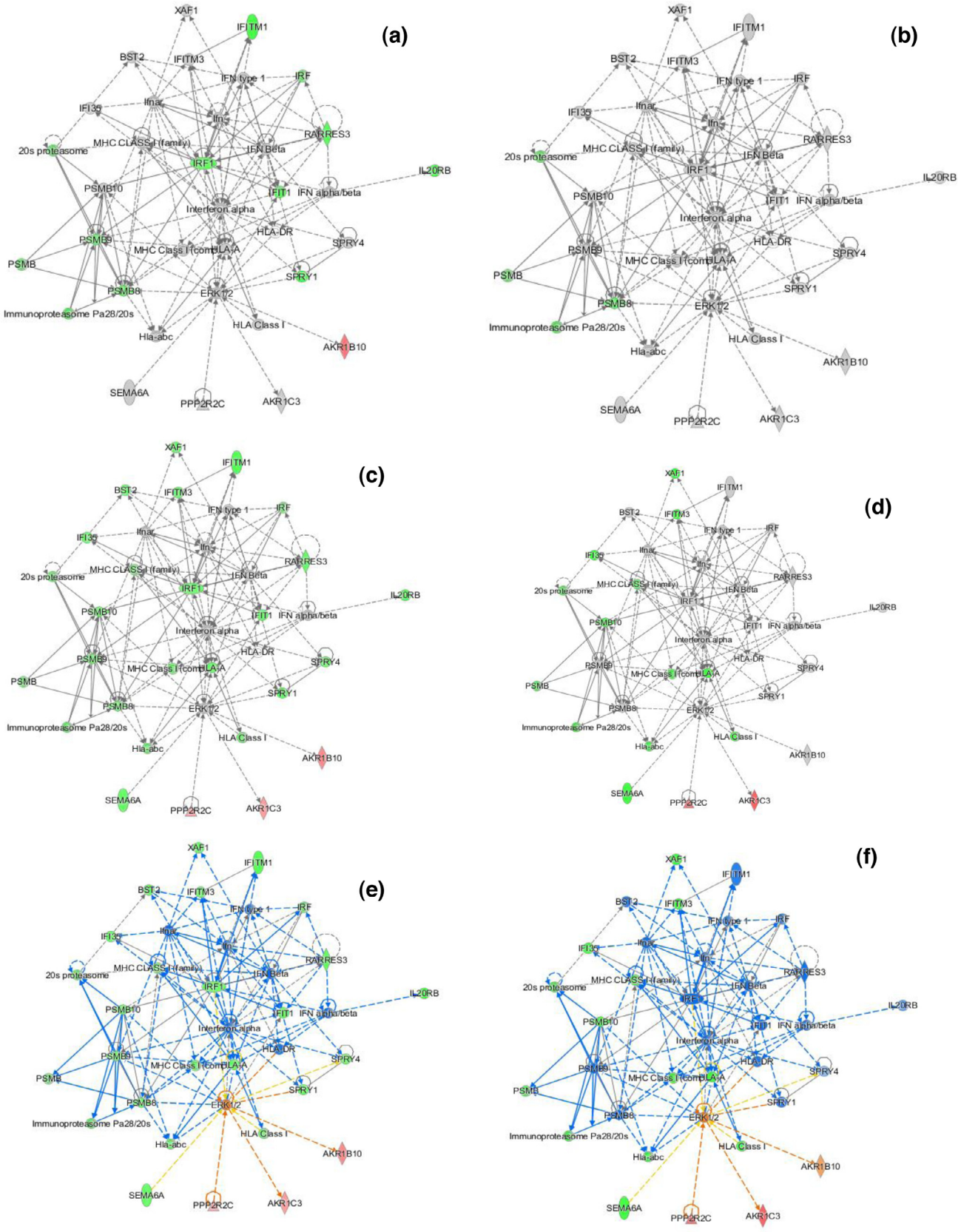

Fig. 5. Effects on molecular network associated with anti-inflammatory and antimicrobial response and cancer: (a) APE, (b) ESE and (c) KJ; (d) shows new synergy-derived elements of KJ signature, (e) and (f) predicted effects.

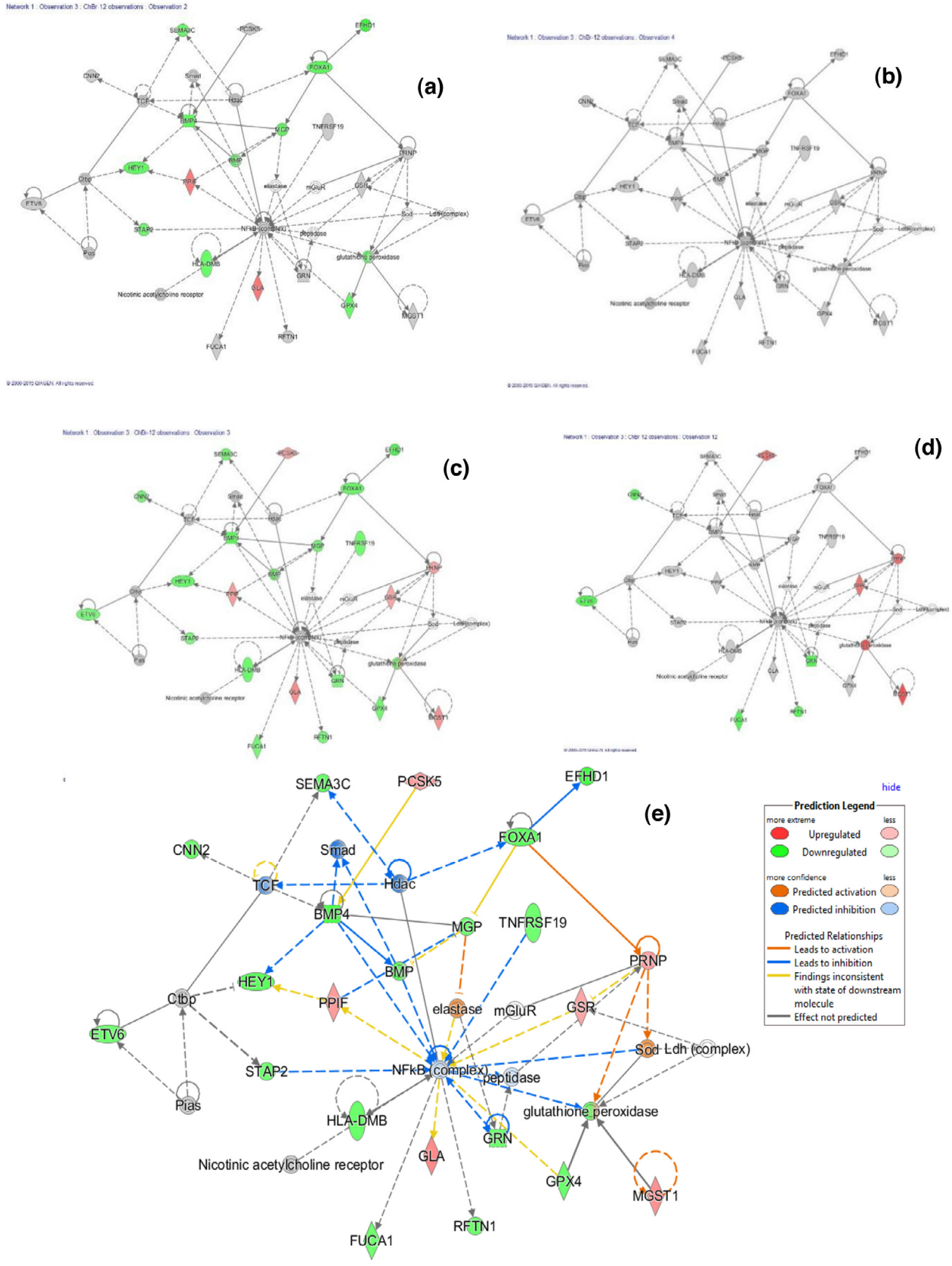

Fig. 6. Effects on molecular networks associated with cellular development, nervous system development and functions: (a) APE, (b) ESE and (c) KJ; (d) shows new synergy-derived elements of KJ signature, (e) predicted effects.

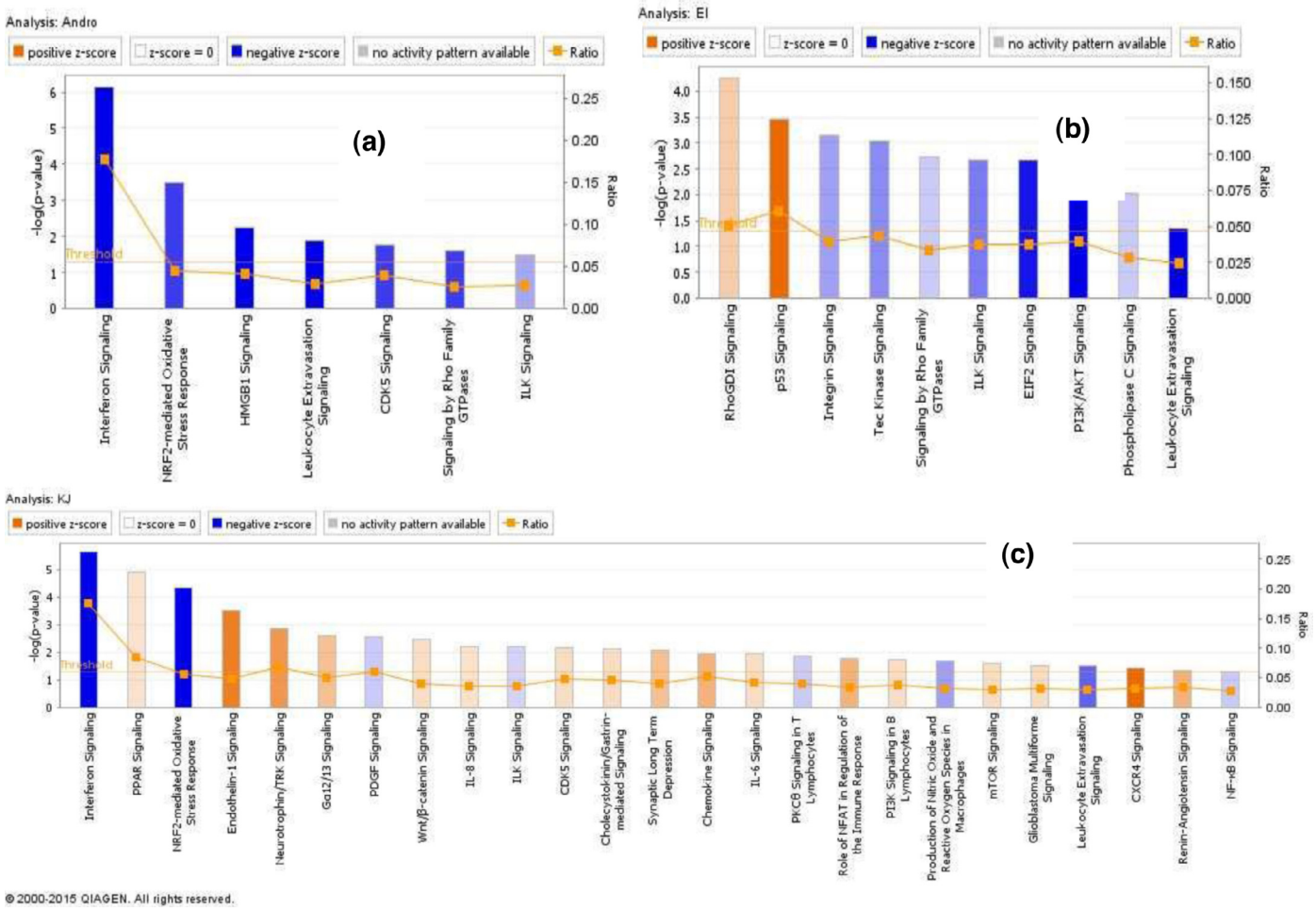

Fig. 7. The most significantly affected canonical pathways: (a) APE, (b) ESE, (c) KJ.

as well as physiological, cellular functions and associated diseases (Fig. 3a–d).

As an example of synergistic interactions in a molecular network, we found that ESE alone has no effect on that network, while KJ deregulated 11 genes with predictable inhibitory effect on infection, while APE regulated only 5 genes, which are activated in encephalitis. It might be speculated that APE in combination with ESE may have better therapeutic effect, since more targets are affected.

Similar observations were made for other networks including significantly affected ($p < 0.05$; $-\log = 1.3$) networks with the predictable (Z-score > 2) effects in infectious and chronic inflammatory disorders (Fig. 5) and neurological movement disorder (Fig. 6) at a significance level of $p < 0.05$ ($-\log = 1.3$) and a Z-score of >2.

Downstream effects analyses of deregulated sets of genes by Ingenuity Pathway Analysis (IPA) software and predicted effects of KJ on cellular and physiological functions and associated deceases

As a next step, we focused on downstream effect analyses of deregulated sets of genes by IPA software with the purpose to uncover molecular targets of APE, ESE, KJ and andrographolide, the main active constituents of APE. We investigated the signaling pathways and molecular networks, which they regulate, and estimated their predictable effects on physiological and cellular functions and associated diseases.

The most significantly affected canonical pathways deregulated by KJ and APE were interferon-signaling and NRF2-mediated oxidative stress response pathways (Fig. 7). Inhibition of NRF2-mediated oxidative stress response is in line with many publications, where anti-inflammatory and antioxidant effects of APE and ESE were demonstrated (Panossian and Wikman 2012; Herba Andrographidis 2002; Radix Eleutherococci 2002).

The predicted inhibition of the interferon-signaling pathway by KJ and APE was due to significant downregulation of six genes: *IFI35, IFIT1, IFITM1, IFITM3, IRF1, PSMB8* encoding interferon-induced protein 35, interferon-induced protein with tetratricopeptide repeats 1, interferon induced transmembrane protein 1, interferon induced transmembrane protein 3, interferon regulatory factor 1, and proteasome subunit beta type 8, respectively. On the other hand, ESE downregulated *JAK1*, which encodes Janus kinase 1, which is upstream of the interferon-signaling cascade (Fig. 8).

The predicted (Z-score > 2) effects in encephalitis (Fig. 4 and "Supplementary" Table 4), and neurological movement disorder (Fig. 6 and "Supplementary" Table 3) are based on changes of gene expression in the experimental samples relative to the control.

Discussion

How to detect synergistic and antagonistic interactions of herbal combinations extracts by DNA microarray hybridization?

Two-set Venn diagrams were used in present study for the analysis of fixed combinations of two plant extracts. The combination of three plant extracts can be analyzed by using the tree-set Venn diagram model as previously reported by us (Panossian et al. 2013). As an example, DNA microarray data from our previous study with a

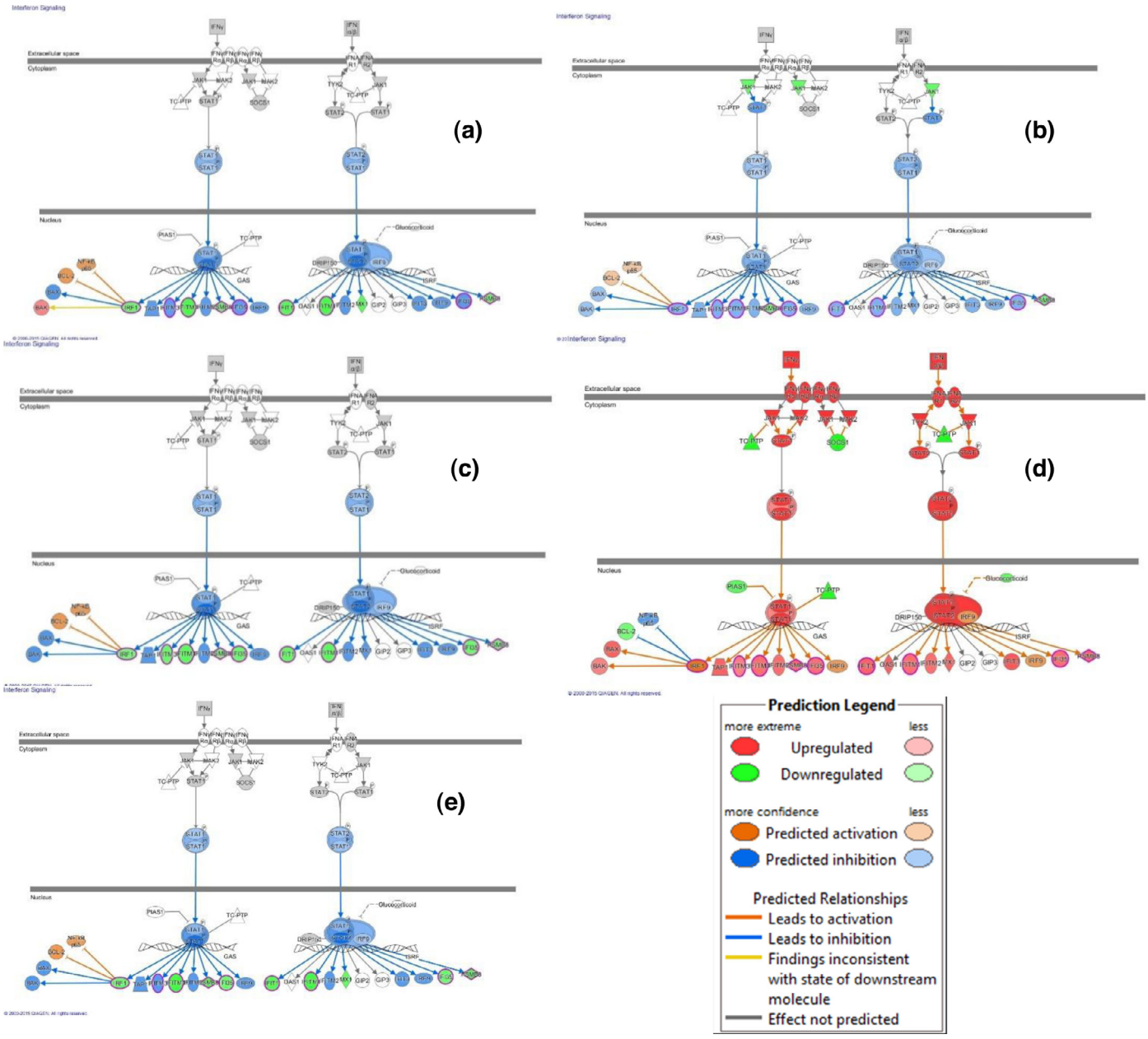

Fig. 8. Activation of the interferon pathway (d) and predicted inhibitory effects of APE (a), ESE (b), KJ (c) and (e) on various steps of this signaling pathway.

combination of three herbs (Panossian et al. 2013) are showed in Fig. 9. The sum of deregulated genes by *Radix Eleutherococci* (ESE), *Schisandra* Fruit (SFE) and *Radix et Rhizome Rhodiola* (RRE) genes is 778 (Fig. 9a). However, their fixed combination (ADAPT) deregulated only 297 genes (Fig. 9b). Among these 297 genes, 86 genes were unique only for the KJ combination and not affected by ESE, SFE and RRE and APE. This is presumably due to synergistic interactions of molecular networks affected by ESE. These 206 genes were deregulated due to synergistic interaction of ingredients. Meanwhile, 241 genes deregulated by ESE, 222 genes deregulated by SFE and 249 genes deregulated by RRE were not deregulated by ADAPT. That is a result of antagonistic integrations of ESE, SFE and RRE extracts, if applied in combination.

The Venn diagrams in Fig. 9 show the number of uniquely deregulated genes for each treatment extract in comparison to the number of commonly deregulated genes.

Unlike to chemical reactions, where the chemical properties of purified compounds remain the same as in their mixture with other chemicals, biological activities of combinations are different from those of their single ingredients (Fig. 3). In fact, it is a "newborn" unique biologically active substance, a hybrid of the "parent" ingredients. The expectations to have a sum of biological activities from two ingredients are elusive. The biological activity of their combination could be qualitatively different.

Peculiarities of KJ fixed combination

Downstream effect analysis of mRNA microarray data enables to predict pharmacological effects of new plant extract combinations on cellular and physiological functions and possible indications for various diseases and finally to conclude, whether an extract combination is really justified.

The most significantly affected canonical pathways deregulated by KJ and APE were interferon-signaling pathways (Figs. 7 and 8). Downregulation of expression of these genes was associated with downregulation of expression of corresponding proteins involved in

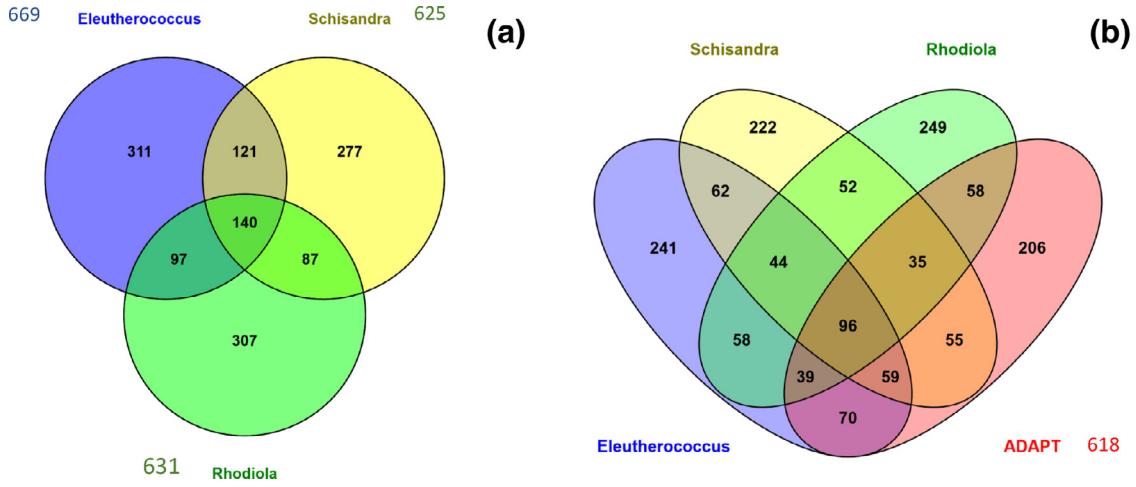

Fig. 9. Venn diagrams of deregulated genes induced by the treatment of neuroglia cells with (a) ESE, SFE and RRE alone and (b) ESE, SFE, RRE in ADAPT. The number of unique genes deregulated by each extract alone (241 by ESE, 222 by SFE and 249 by RRE) and 206 uniquely deregulated genes by ADAPT showed antagonistic and synergistic interactions of ESE, SFE and RRE in ADAPT. Overlapping sections show commonly deregulated genes by these ingredients in the ADAPT combination.

initiating immune responses, especially in antiviral and antitumor effects. Inhibition of IFN-gamma signaling pathways may represent an appropriate treatment goal, if interferon is overproduced, *e.g.* in sepsis (Dejager et al. 2014) and various autoimmune diseases, including skin diseases rheumatoid arthritis, multiple sclerosis, corneal transplant rejection, and various autoimmune skin diseases such as psoriasis, alopecia areata, vitiligo, acne vulgaris, systemic lupus erythematosus, and others (Skurkovich and Skurkovich 2006; Lateef and Petria 2010).

Upstream effect analysis showed inhibition of IFN-α, IFN-β, IFNB1 and IFNG by KJ and APE that is in line with several studies with isolated cells (Burgos et al. 2005; Parichatikanond et al. 2010), but in contradiction with the results of few others *in vitro* (Panossian et al. 2002; Denzler et al. 2010) and *in vivo* studies, where the immunostimulatory effect of *Andrographis* was demonstrated (Puri et al. 1993). An explanation of contradictory results might be due to differences in test systems (isolated cell lines, whole blood and experiments *in vivo*), various concentrations and presence of the bacterial LPS in Herba Andrographidis extracts (Denzler et al. 2010). Many immunostimulatory extracts appear to contain LPS, likely from the lysis of endophytic bacteria, which have been identified in the tissues of every living plant known (Strobel and Daisy 2003; Rosenblueth and Martinez-Romero 2006). It can be speculated that low concentrations of APE cause immunostimulatory LPS effects, while at higher concentrations inhibitory effects of andrographolide and other *Andrographis paniculata* secondary metabolites are dominant.

The results of this study clearly show that the KJ combination is potentially more active than APE or ESE to inhibit IFN signaling and presumably more efficient to treat diseases associated with interferon overexpression.

Synergy derived predicted beneficial effects of the KJ combination may be expected in encephalitis and neurological movement disorders.

Though, microarray analysis did not provide a final proof that the genes induced by KJ, APE and ESE are indeed responsible for the physiological effects observed in humans following their oral administration, it provided insights into putative genetic signaling pathways for future research and possible implementation into practice.

Conclusions

Analysis of mRNA microarray data from neuroglial T98G cells and the comparison profiles of genes regulated by plant extracts and their fixed herbal formulation might be a useful method for the assessment of synergistic and antagonistic interactions of herbal extracts in human organism. Downstream effect analysis of mRNA microarray data enables to predict, whether a combination of various extracts is justified. We conclude that the combination of APE and ESE in KJ formulation is most likely justified.

Conflicts of interest

E.-J.S., T.E., and A.P. declare not to have competing financial interests. G.W. is a stockholder in the Swedish Herbal Institute (SHI).

Supplementary Materials

Supplementary material associated with this article can be found, in the online version, at doi:10.1016/j.phymed.2015.08.004.

References

Amaryan, G., Astvatsatryan, V., Gabrielyan, E., Panossian, A., Panosyan, V., Wikman, G., 2003. Double-blind, placebo-controlled, randomized, pilot clinical trial of Immuno-Guard® - a standardized fixed combination of *Andrographis paniculata* Nees, with *Eleutherococcus senticosus* Maxim, *Schizandra chinensis* Bail. and *Glycyrrhiza glabra* L. extracts in patients with Familial Mediterranean Fever. Phytomedicine 10, 271–285.

Burgos, R.A., Seguel, K., Perez, M., Meneses, A., Ortega, M., Guarda, M.I., Loaiza, A., Hancke, J.L., 2005. Andrographolide inhibits IFN-gamma and IL-2 cytokine production and protects against cell apoptosis. Planta Med. 71, 429–434.

Dejager, L., Vandevyver, S., Ballegeer, M., Van Wonterghem, E., An, L.L., Riggs, J., Kolbeck, R., Libert, C., 2014. Pharmacological inhibition of type I interferon signaling protects mice against lethal sepsis. J. Infect. Dis. 209, 960–970.

Denzler, K.L., Waters, R., Jacobs, B.L., Rochon, Y., Langland, J.O., 2010. Regulation of inflammatory gene expression in PBMCs by immunostimulatory botanicals. PLoS One 5 (e12561), 1–15.

Efferth, T., Koch, E., 2011. Complex interactions between phytochemicals. The multitarget therapeutic concept of phytotherapy. Curr. Drug Targ. 12, 122–132.

ESCOP Monographs, 2003. Eleutherococci Radix: The Scientific Foundation of Herbal Medicinal Products, 2nd ed.. In: European Scientific Cooperative Phytotherapy (ESCOP) Monographs. European Scientific Cooperative on Phytotherapy and Thieme, Exeter (UK), pp. 142–149.

Farnsworth, N.R., Kinghorn, A.D., Soejarto, D.D., Waller, D.P., 1985. Siberian ginseng (*Eleuherococcus senticosus*): current status as an adaptogen. In: Wagner, H., Hikino, H., Farnsworth, N.R. (Eds.), Economic and Medicinal Plant Research, vol. 1. Academic Press, London, pp. 155–215.

Gabrielian, E.S., Shukarian, A.K., Goukasova, G.I., Chandanian, G.L., Panossian, A.G., Wikman, G., Wagner, H., 2002. A double blind, placebo-controlled study of *Andrographis paniculata* fixed combination Kan Jang in the treatment of acute upper respiratory tract infections including sinusitis. Phytomedicine 9, 589–597.

Herba Andrographidis, 2002. WHO Monographs on Selected Medicinal Plants, vol. 2. WHO, Geneva, pp. 12–24 2002.

Herba Andrographis (Chuanxinlian), 2010. Pharmacopoeia of the People's Republic of China 2010 (English Ed.), vol. 1. China Medical Science Press, Beijing, China, pp. 32–33.

Kulichenko, L.L., Kireyeva, L.V., Malyshkina, E.N., Wikman, G., 2003. A randomized, controlled study of Kan Jang versus amantadine in the treatment of influenza in Volgograd. J. Herb. Pharmacother. 3, 77–93.

Lateef, A., Petria, M., 2010. Biologics in the treatment of systemic lupus erythematosus. Curr. Opin. Rheumatol. 22, 504–509.

Panossian, A., Hovhannisyan, A., Mamikonyan, G., Abrahamian, H., Hambardzumyan, E., Gabrielian, E., Goukasova, G., Wikman, G., Wagner, H., 2000. Pharmacokinetic and oral bioavailability of andrographolide from *Andrographis paniculata* fixed combination Kan Jang in rats and human. Phytomedicine 7, 351–364.

Panossian, A., Davtyan, T., Gukassyan, N., Gukasova, G., Mamikonyan, G., Gabrielyan, E., Wikman, G., 2002. Effect of andrographolide and Kan Jang – fixed combination of extract SHA-10 and extract SHE-3 – on proliferation of human lymphocytes, production of cytokines and immune activation markers in the whole blood cells culture. Phytomedicine 90, 598–605.

Panossian, A., Hamm, R., Kadioglu, O., Wikman, G., Efferth, T., 2013. Synergy and antagonism of active constituents of ADAPT-232 on transcriptional level of metabolic regulation of isolated neuroglial cells. Front Neurosci 7, 16 http://journal.frontiersin.org/article/10.3389/fnins.2013.00016/abstract .

Panossian, A., Wikman, G., 2012. Efficacy *of Andrographis paniculata* in upper respiratory tract (URT) infectious diseases and the mechanism of action. In: Wagner, H., Ulrich Merzenich, G. (Eds.), Evidence and Rational Based Research on Chinese Drugs. Springer, pp. 137–180.

Parichatikanond, W., Suthisisang, C., Dhepakson, P., Herunsalee, A., 2010. Study of anti-inflammatory activities of the pure compounds from *Andrographis paniculata* (burm. f.) Nees and their effects on gene expression. Int. Immunopharmacol. 10, 1361–1373.

Puri, A., Saxena, R., Saxena, R.P., Saxena, K.C., Srivastava, V., Tandon, J.S., 1993. Immunostimulant agents from *Andrographis paniculata*. J. Nat. Prod. 56, 995–999.

Radix Eleutherococci, 2002. WHO Monographs on Selected Medicinal Plants, vol. 2. WHO, Geneva, pp. 83–96 2002.

Radix et, Rhizoma seu Caulis Acanthopanacis Senticosi (Ciwaujia), 2005. Pharmacopoeia of the People's Republic of China 2005 (English Ed.), 1. People's Medical Publishing House, Beijing, China, p. 121.

Rosenblueth, M., Martinez-Romero, E., 2006. Bacterial endophytes and their interactions with hosts. Mol. Plant Microbe Interact. 19, 827–837.

Skurkovich, B., Skurkovich, S., 2006. Inhibition of IFN-gamma as a method of treatment of various autoimmune diseases, including skin diseases. Ernst Schering Res. Found. Workshop. 56, 1–27.

Strobel, G., Daisy, B., 2003. Bioprospecting for microbial endophytes and their natural products. Microbiol. Mol. Biol. Rev. 67, 491–502.

Wagner, H., 2006. Multitarget therapy—the future of treatment for more than just functional dyspepsia. Phytomedicine. 5, 122–129.